BAMS Supplement

The NASA Atmospheric Tomography (ATom) Mission

Imaging the Chemistry of the Global Atmosphere

Chelsea R. Thompson, Steven C. Wofsy, Michael J. Prather, Paul A. Newman, Thomas F. Hanisco, Thomas B. Ryerson, David W. Fahey, Eric C. Apel, Charles A. Brock, William H. Brune, Karl Froyd, Joseph M. Katich, Julie M. Nicely, Jeff Peischl, Eric Ray, Patrick R. Veres, Siyuan Wang, Hannah M. Allen, Elizabeth Asher, Huisheng Bian, Donald Blake, Ilann Bourgeois, John Budney, T. Paul Bui, Amy Butler, Pedro Campuzano-Jost, Cecilia Chang, Mian Chin, Róisín Commane, Gus Correa, John D. Crounse, Bruce Daube, Jack E. Dibb, Joshua P. DiGangi, Glenn S. Diskin, Maximilian Dollner, James W. Elkins, Arlene M. Fiore, Clare M. Flynn, Hao Guo, Samuel R. Hall, Reem A. Hannun, Alan Hills, Eric J. Hintsa, Alma Hodzic, Rebecca S. Hornbrook, L. Greg Huey, Jose L. Jimenez, Ralph F. Keeling, Michelle J. Kim, Agnieszka Kupc, Forrest Lacey, Leslie R. Lait, Jean-Francois Lamarque, Junhua Liu, Kathryn McKain, Simone Meinardi, David O. Miller, Stephen A. Montzka, Fred L. Moore, Eric J. Morgan, Daniel M. Murphy, Lee T. Murray, Benjamin A. Nault, J. Andrew Neuman, Louis Nguyen, Yenny Gonzalez, Andrew Rollins, Karen Rosenlof, Maryann Sargent, Gregory Schill, Joshua P. Schwarz, Jason M. St. Clair, Stephen D. Steenrod, Britton B. Stephens, Susan E. Strahan, Sarah A. Strode, Colm Sweeney, Alexander B. Thames, Kirk Ullmann, Nicholas Wagner, Rodney Weber, Bernadett Weinzierl, Paul O. Wennberg, Christina J. Williamson, Glenn M. Wolfe, and Linghan Zeng

https://doi.org/10.1175/BAMS-D-20-0315.2
Corresponding author: Chelsea R. Thompson, chelsea.thompson@noaa.gov
This is a supplement to https://doi.org/10.1175/BAMS-D-20-0315.1

AFFILIATIONS: **Thompson, Froyd, Katich, Peischl, Ray, Bourgeois, Neuman, Schill, Wagner, and Williamson**—NOAA Chemical Sciences Laboratory, and University of Colorado Boulder, Boulder, Colorado; **Ryerson, Fahey, Brock, Veres, Butler, Murphy, Rollins, Rosenlof, and Schwarz**—NOAA Chemical Sciences Laboratory, Boulder, Colorado; **Wofsy, Budney, Commane,* Daube, Gonzalez, and Sargent**—Harvard University, Cambridge, Massachusetts; **Prather, Blake, Flynn,* Guo, and Meinardi**—University of California, Irvine, Irvine, California; **Newman, Hanisco, Chin, and Wolfe**—NASA Goddard Space Flight Center, Greenbelt, Maryland; **Nicely**—NASA Goddard Space Flight Center, Greenbelt, and University of Maryland, College Park, College Park, Maryland; **Apel, Wang,* Asher,* Hall, Hills, Hodzic, Hornbrook, Lacey, Lamarque, Stephens, and Ullmann**—National Center for Atmospheric Research, Boulder, Colorado; **Brune, Miller, and Thames**—The Pennsylvania State University, University Park, Pennsylvania; **Allen, Crounse, Kim, and Wennberg**—California Institute of Technology, Pasadena, California; **Bian, Hannun, and St. Clair**—NASA Goddard Space Flight Center, Greenbelt, and University of Maryland, Baltimore County, Baltimore, Maryland; **Bui and Chang**—NASA Ames Research Center, Mountain View, California; **Campuzano-Jost, Jimenez, and Nault***—University of Colorado Boulder, Boulder, Colorado; **Correa and Fiore**—Columbia University, Palisades, New York; **Dibb**—University of New Hampshire, Durham, New Hampshire; **DiGangi, Diskin, and Nguyen**—NASA Langley Research Center, Hampton, Virginia; **Dollner and Weinzierl**—University of Vienna, Vienna, Austria; **Elkins, Montzka, and Sweeney**—NOAA Global Monitoring Laboratory, Boulder, Colorado; **Hintsa, McKain, and Moore**—NOAA Global Monitoring Laboratory, and University of Colorado Boulder, Boulder, Colorado; **Huey, Weber, and Zeng**—Georgia Institute of Technology, Atlanta, Georgia; **Keeling and Morgan**—Scripps Institution of Oceanography, La Jolla, California; **Kupc**—NOAA Chemical Sciences Laboratory, Boulder, Colorado, and University of Vienna, Vienna, Austria; **Lait**—NASA Goddard Space Flight Center, Greenbelt, and Science Systems and Applications, Inc., Lanham, Maryland; **Liu, Steenrod, Strahan, and Strode**—NASA Goddard Space Flight Center, Greenbelt, and Universities Space Research Association, Columbia, Maryland; **Murray**—University of Rochester, Rochester, New York
CURRENT AFFILIATIONS: Commane—Columbia University, Palisades, New York; **Flynn**—Stockholm University, Stockholm, Sweden; **Wang and Asher**—NOAA Chemical Sciences Laboratory, and University of Colorado Boulder, Boulder, Colorado; **Nault**—Aerodyne Research Inc., Billerica, Massachusetts

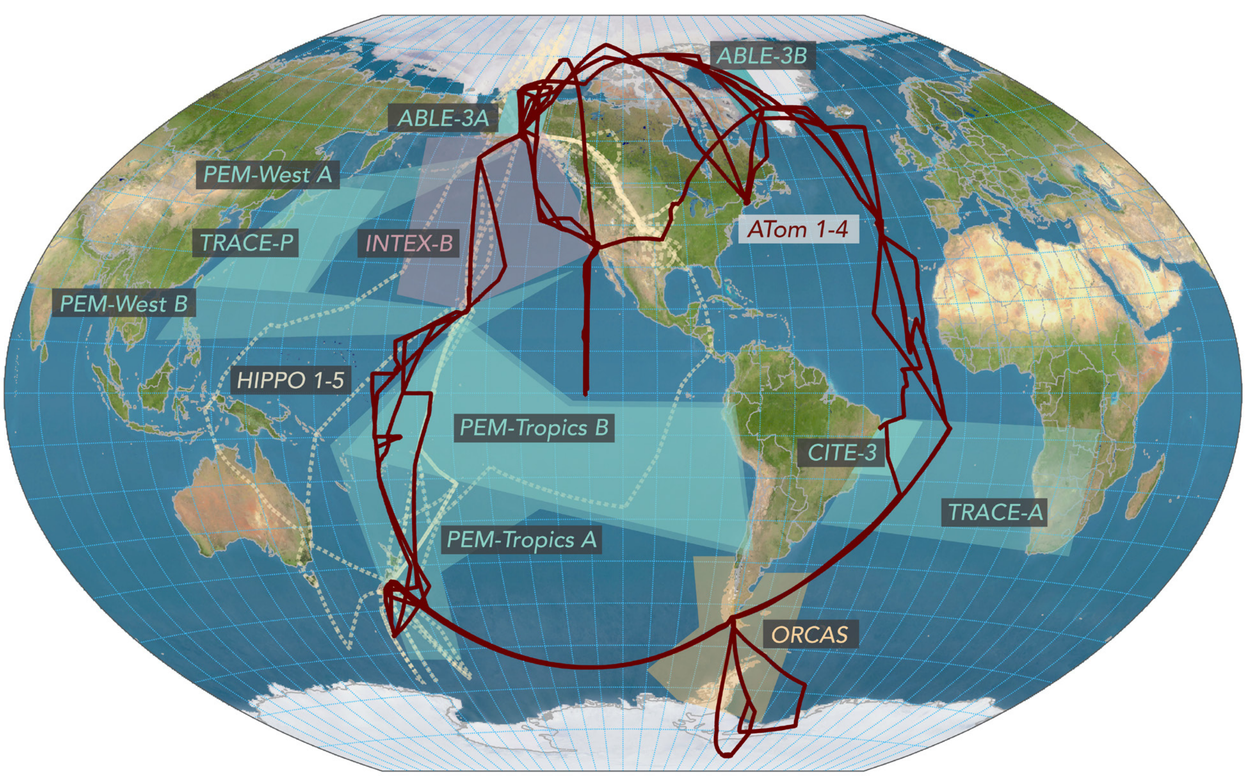

Fig. ES1. Map of the ATom flight tracks in relation to flights conducted in previous relevant airborne campaigns. The missions shown in aqua are part of the NASA Global Tropospheric Experiment (GTE) series.

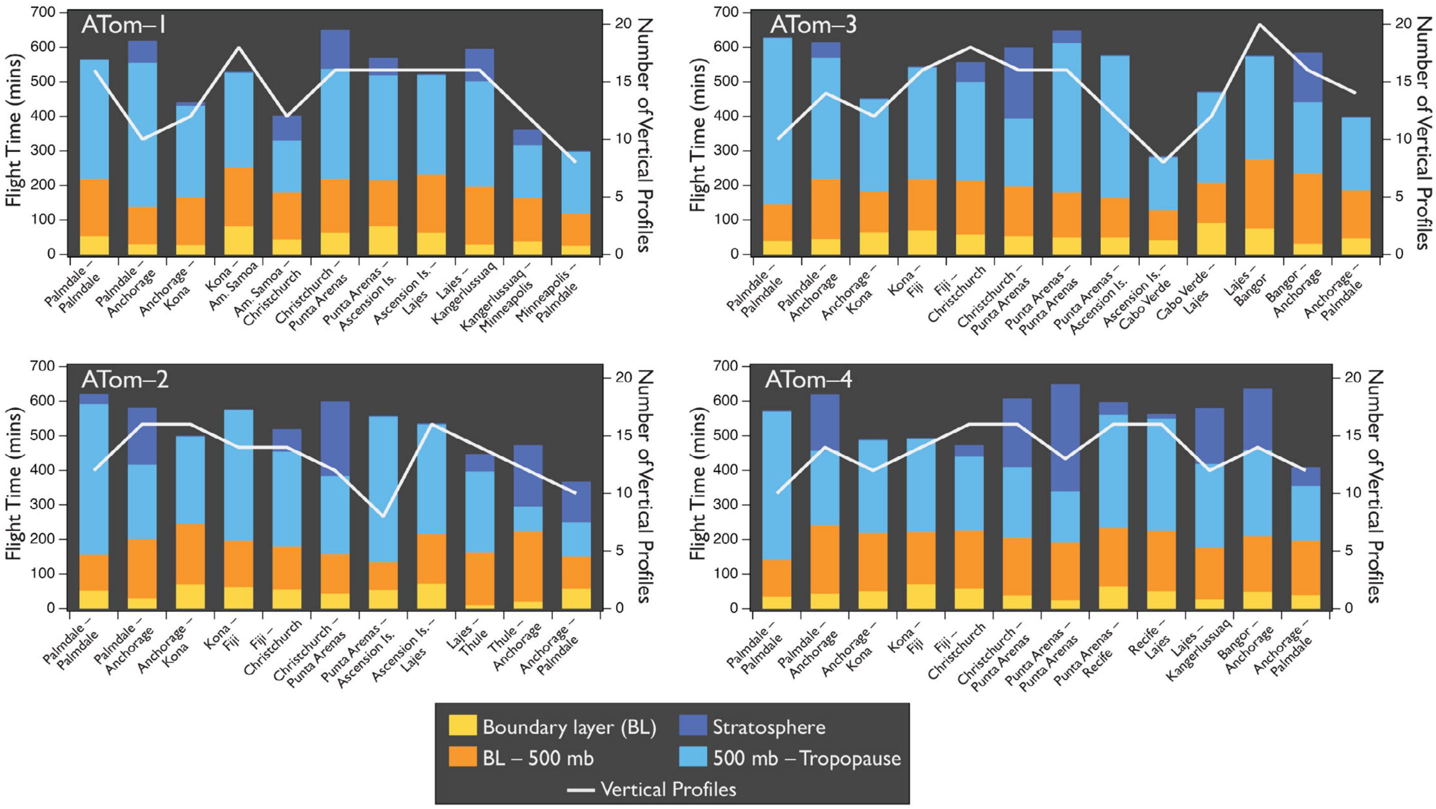

Fig. ES2. Cumulative flight time for each research flight, subdivided by time spent within the boundary layer, boundary layer to 500-mb pressure altitude, 500 mb to the tropopause, and the stratosphere. The white trace indicates the total number of vertical profiles performed for each research flight.

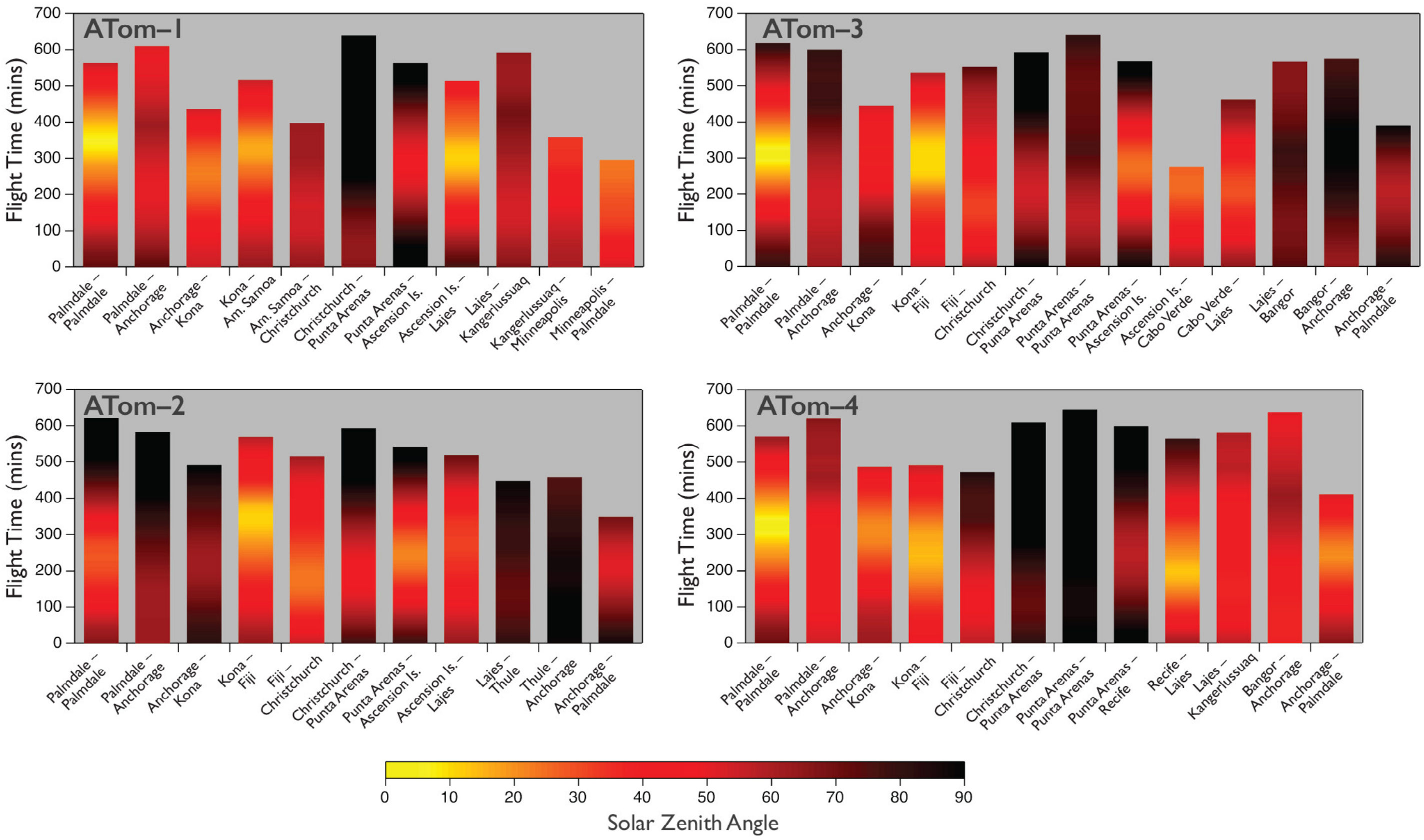

Fig. ES3. Total flight time for each research flight of the four ATom deployments, colored by solar zenith angle. The bars are oriented such that the bottom of the bar (time 0) is the aircraft takeoff time and the top of the bar is the aircraft landing time for each flight.

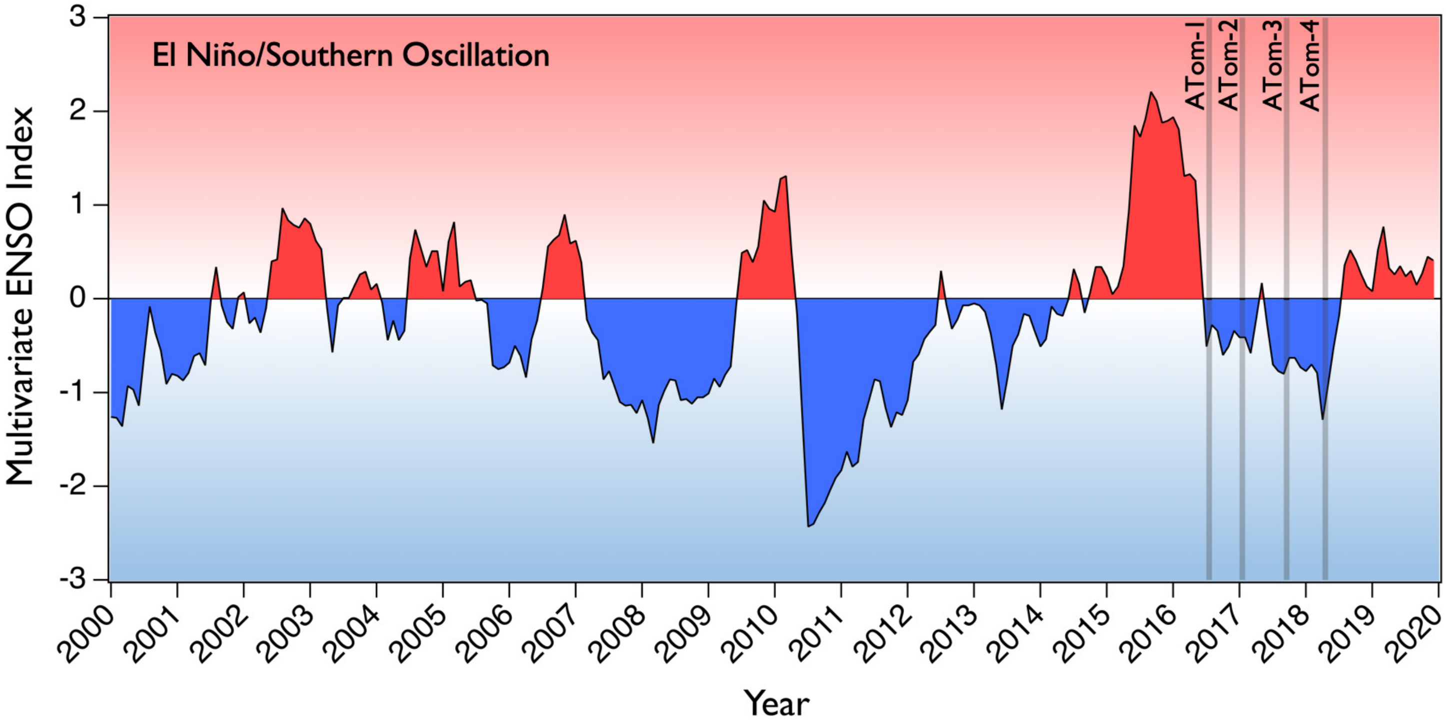

Fig. ES4. The 20-yr historical trend of the multivariate El Niño–Southern Oscillation index with the time periods of the four ATom deployments noted.

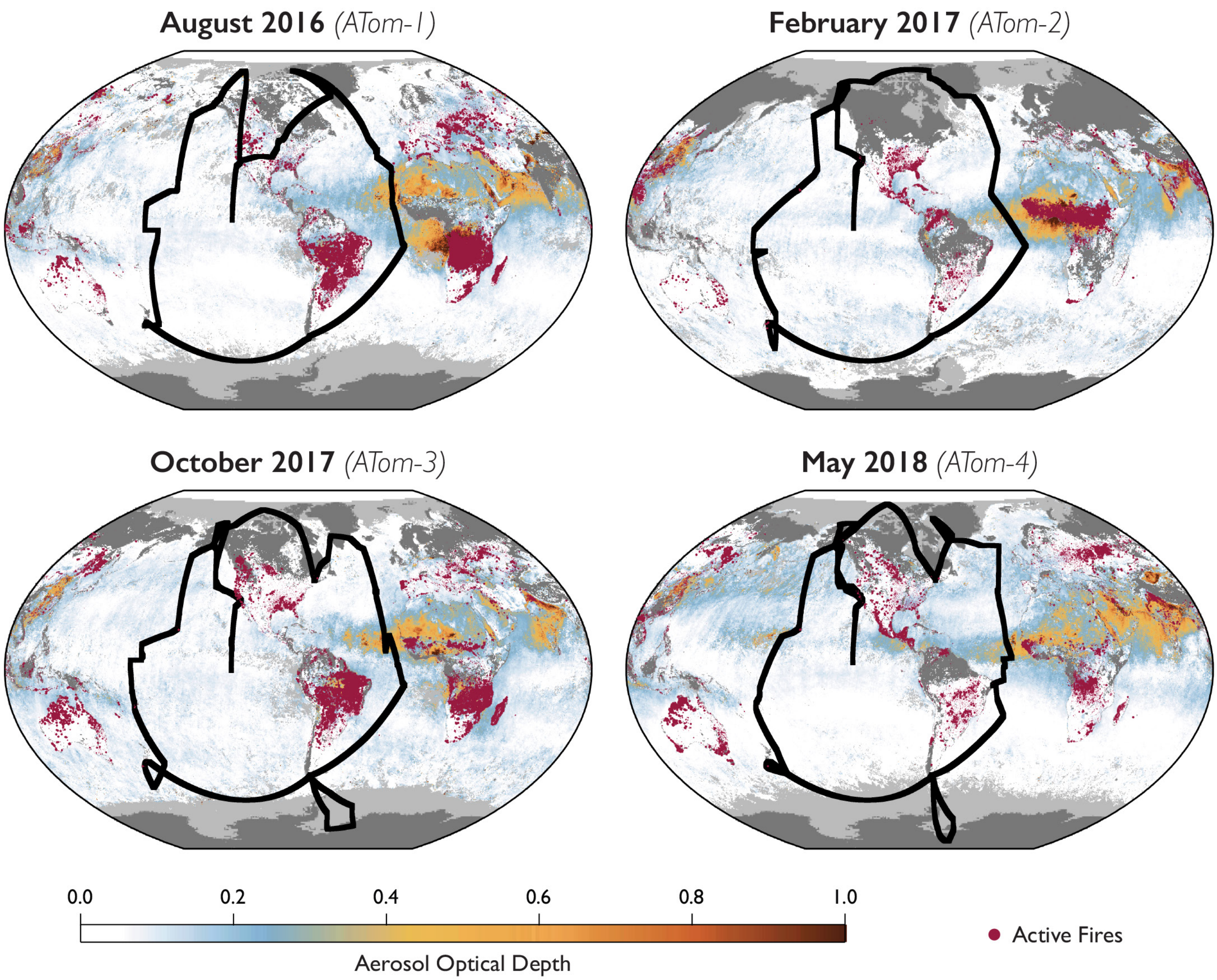

Fig. ES5. Maps of monthly average aerosol optical depth (AOD) and monthly aggregated fires during the four ATom deployments. AOD and fire location data are based on observations from the MODIS instrument on board NASA's *Terra* satellite. The ATom flight tracks are indicated by the black traces.

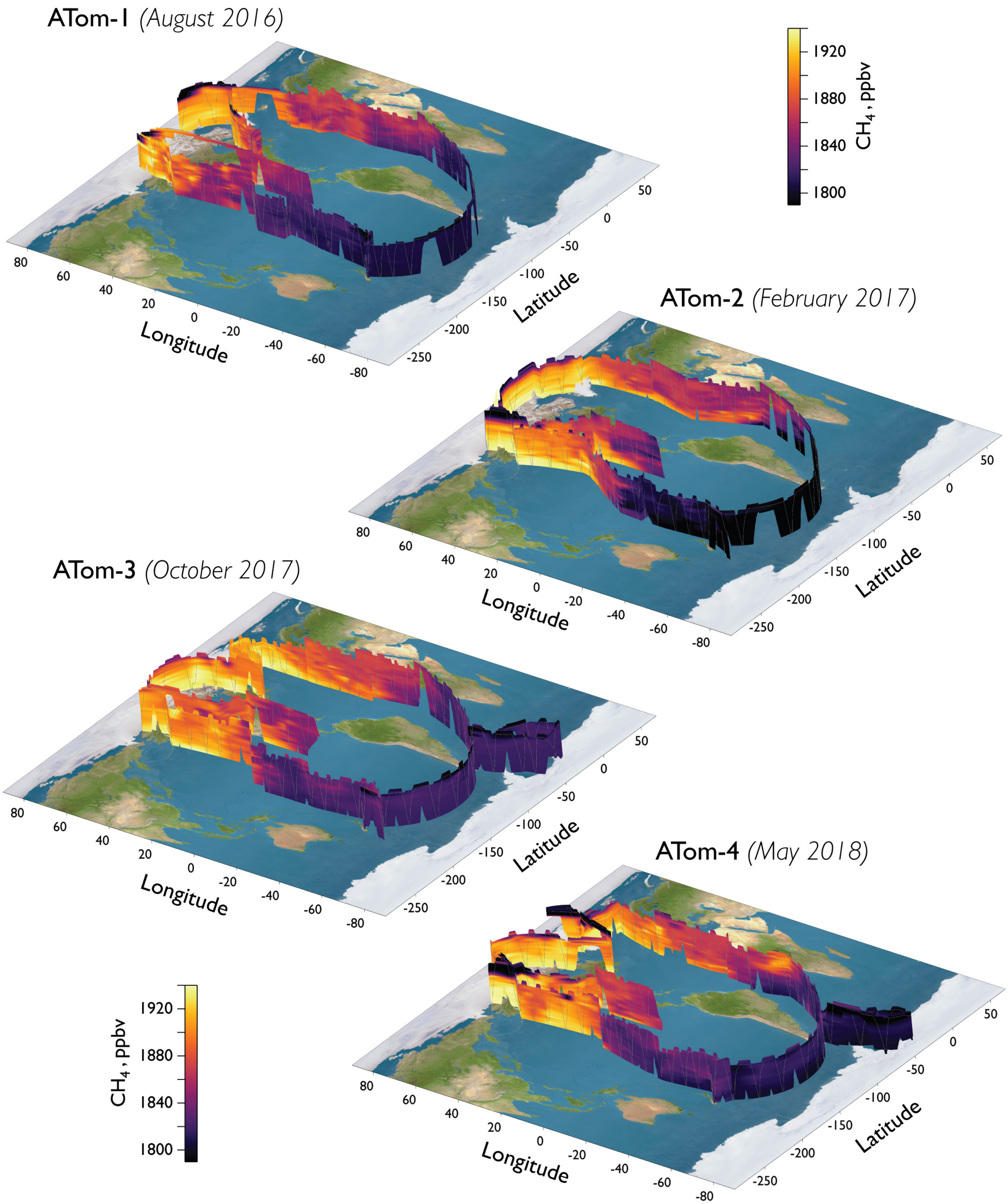

Fig. ES6. Curtain plots showing CH_4 for all four deployments interpolated from measurements collected along the ATom-1, -2, -3, and -4 flight tracks.

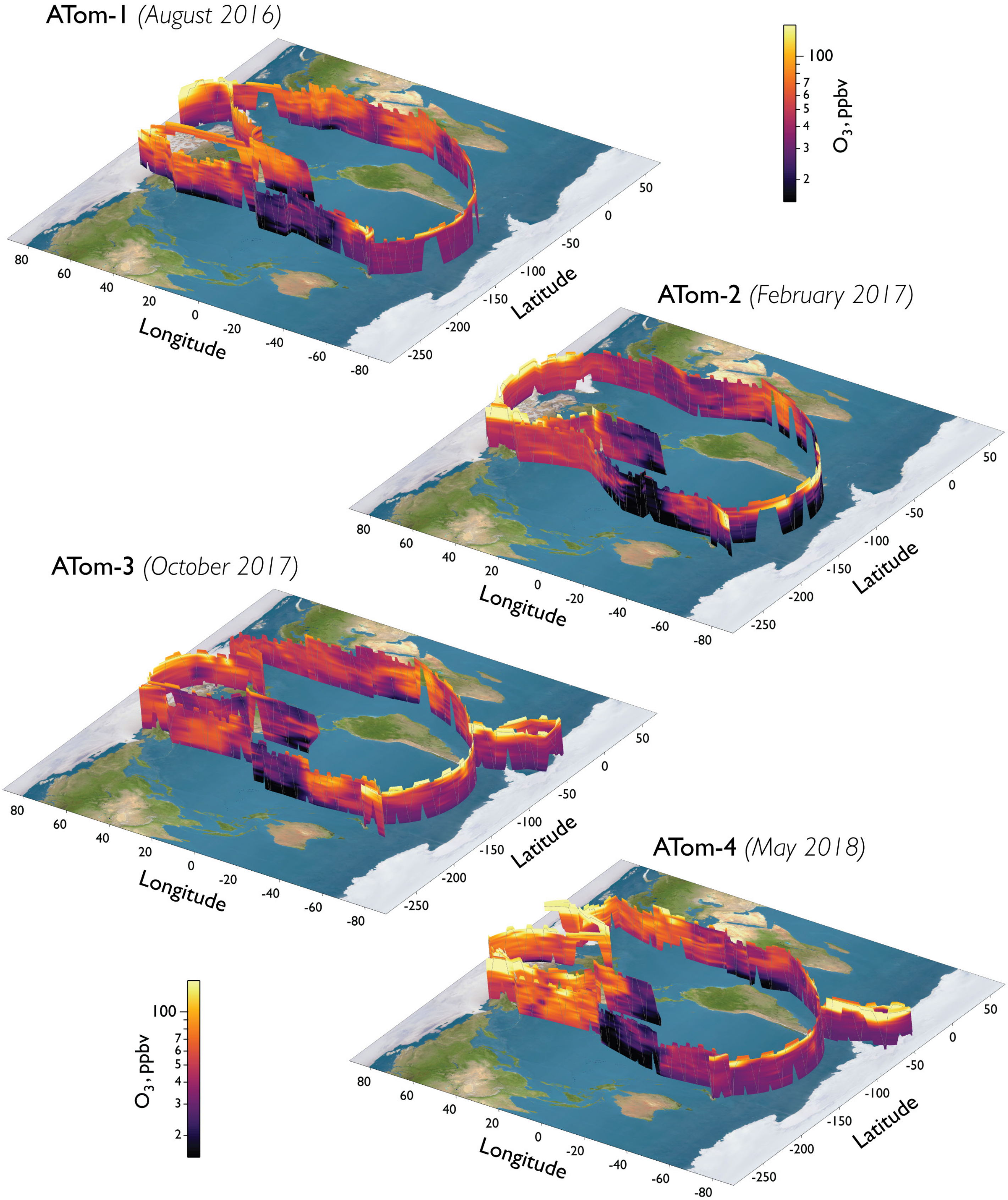

Fig. ES7. Curtain plots showing O_3 for all four deployments interpolated from measurements collected along the ATom-1, -2, -3, and -4 flight tracks. Note that O_3 mixing ratio is shown on a log scale.

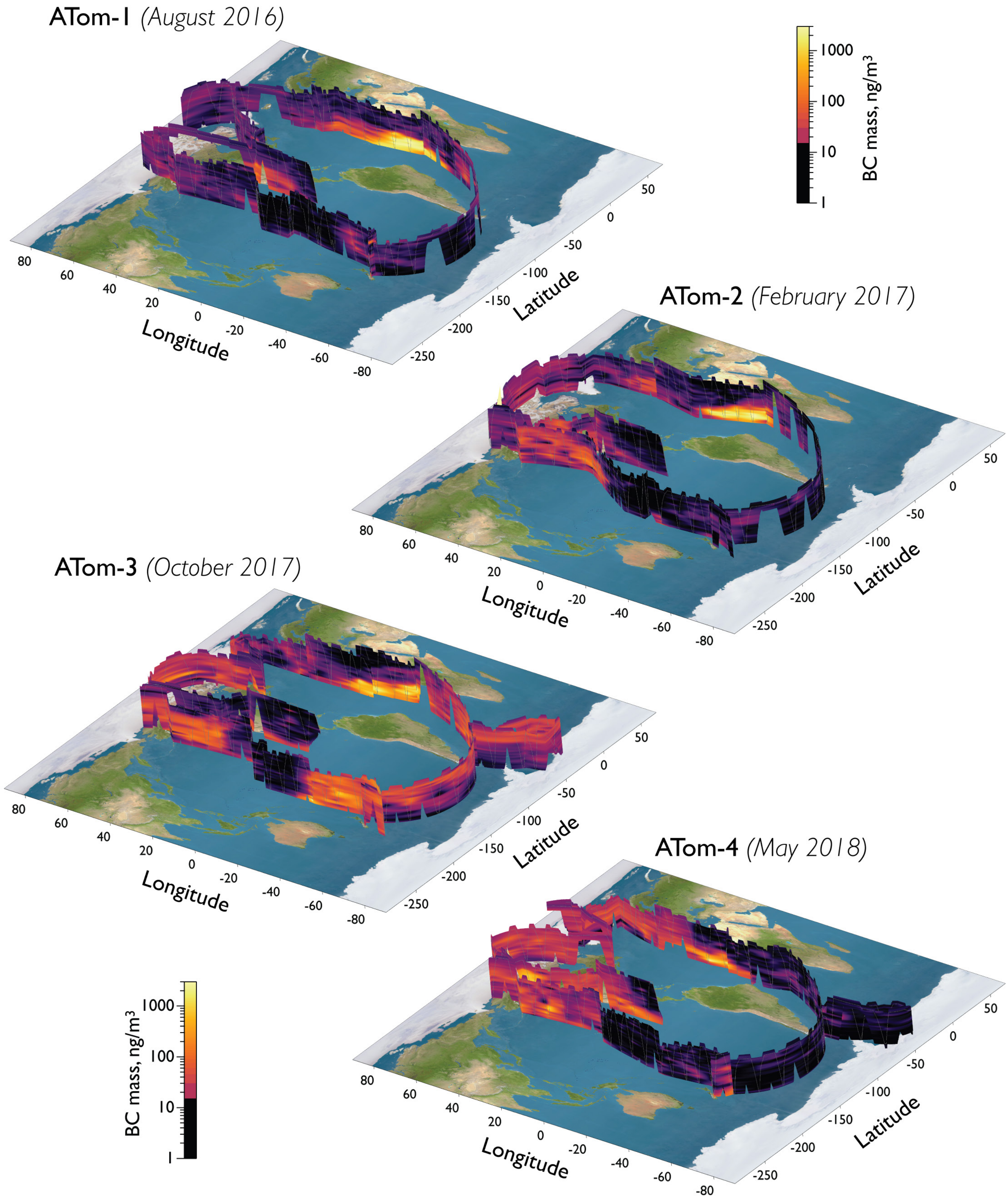

Fig. ES8. Curtain plots showing BC for all four deployments interpolated from measurements collected along the ATom-1, -2, -3, and -4 flight tracks. Note that BC mass is shown on a log scale.

Table ES1. Summary of previous airborne missions relevant to ATom.

Expedition	Date	Location	Platform
CITE-1B	Nov 1983	Hawaii	NASA DC-8
ABLE-3A	Jul 1988	Alaska	NASA DC-8
CITE-3	Aug 1989	Atlantic, Virginia, and Brazil	NASA DC-8
ABLE-3B	Jul 1990	Canada	NASA DC-8
PEM-West A	Oct 1991	Western Pacific	NASA DC-8
TRACE-A	Sep 1992	Brazil, South Atlantic, southwestern Africa	NASA DC-8
PEM-West B	Feb 1994	Western Pacific	NASA DC-8
PEM-Tropics A	Aug 1996	Tropical Pacific	NASA DC-8
PEM-Tropics B	Mar 1999	Tropical Pacific	NASA DC-8
TRACE-P	Feb 2001	Western Pacific	NASA DC-8
INTEX-B/Part II	Apr 2006	Central Pacific	NASA DC-8
HIPPO 1	Jan 2009	Pole-to-pole Pacific basin	NCAR/NSF GV
HIPPO 2	Nov 2009	Pole-to-pole Pacific basin	NCAR/NSF GV
HIPPO 3	Mar–Apr 2010	Pole-to-pole Pacific basin	NCAR/NSF GV
HIPPO 4	Jun–Jul 2011	Pole-to-pole Pacific basin	NCAR/NSF GV
HIPPO 5	Aug–Sep 2011	Pole-to-pole Pacific basin	NCAR/NSF GV
ORCAS	Jan–Feb 2016	Southern Ocean, Drake Passage	NCAR/NSF GV

Table ES2. Individual flight details for the ATom research flights. Dates are shown in MM/DD/YY format; times are shown in HH:MM format.

Flight No.	Location	Takeoff date and time (UTC)	Landing date and time (UTC)	Distance (km)	Cumulative distance (km)	Latitude range	Longitude range	Altitude range (km)	No. of profiles
ATom-1									
1	Palmdale–equator–Palmdale	07/29/16 14:33	07/29/16 23:56	6,912	6,912	4.96° to 34.71°	−120.73° to −117.86°	0.168–12.7	16
2	Palmdale–Anchorage	08/01/16 14:29	08/02/16 00:39	7,498	14,410	34.63° to 79.25°	−150.43° to −118.11°	0.0771–11.5	10
3	Anchorage–Kona	08/03/16 19:00	08/04/16 02:17	5,057	19,467	19.74° to 61.29°	−162.89° to −150.01°	0.166–13.2	12
4	Kona–Pago Pago	08/06/16 17:57	08/07/16 02:34	6,309	25,776	−14.44° to 19.73°	−174.08° to −156.05°	0.171–12.0	18
5	Pago Pago–Christchurch	08/08/16 19:34	08/09/16 02:11	4,781	30,557	−45.47° to −14.32°	−190.40° to −170.65°	0.159–11.6	12
6	Christchurch–Punta Arenas	08/12/16 22:15	08/13/16 08:54	7,807	38,364	−65.33° to −43.50°	−187.64° to −70.86°	0.170–11.7	16
7	Punta Arenas–Ascension Island	08/15/16 10:28	08/15/16 19:51	7,213	45,577	−53.08° to −7.77°	−70.98° to −14.39°	0.169–12.6	16
8	Ascension Island–Lajes	08/17/16 08:04	08/17/16 16:36	6,123	51,700	−8.07° to 39.73°	−27.34° to −14.34°	0.171–12.9	16
9	Lajes–Kangerlussuaq	08/20/16 09:03	08/20/16 18:54	7,202	58,902	38.71° to 80.01°	−86.66° to −26.40°	0.166–12.1	16
10	Kangerlussuaq–Minneapolis	08/22/16 12:53	08/22/16 18:51	3,869	62,771	44.88° to 67.00°	−93.47° to −50.76°	0.316–11.9	12
11	Minneapolis–Palmdale	08/23/16 15:05	08/23/16 20:00	3,116	65,887	34.63° to 44.87°	−118.10° to −93.12°	0.389–12.8	8
ATom-2									
1	Palmdale–equator–Palmdale	01/26/17 17:11	01/27/17 3:32	7,827	73,714	0.91° to 34.70°	−121.75° to −118.01°	0.156–12.9	12
2	Palmdale–Anchorage	01/29/17 17:39	01/30/17 03:21	6,869	80,583	34.63° to 71.29°	−157.41° to −118.11°	0.0456–11.3	16
3	Anchorage–Kona	02/01/17 20:09	02/02/17 04:20	5,928	86,511	19.53° to 61.26°	−162.86° to −146.34°	0.0460–10.6	16
4	Kona–Nadi	02/03/17 18:59	02/04/17 04:27	7,074	93,585	−17.96° to 19.73°	−182.81° to −156.05°	0.152–12.0	14
5	Nadi–Christchurch	02/05/17 20:32	02/06/17 05:07	6,250	99,835	−56.06° to −17.77°	−195.42° to −179.17°	0.147–12.3	14
6	Christchurch–Punta Arenas	02/10/17 18:54	02/11/17 04:46	7,854	107,689	−65.28° to −43.50°	−187.56° to −70.51°	0.165–12.0	12
7	Punta Arenas–Ascension Island	02/13/17 11:01	02/13/17 20:01	7,208	114,897	−53.00° to −7.76°	−70.97° to −14.40°	0.167–12.6	8
8	Ascension Island–Lajes	02/15/17 08:51	02/15/17 17:29	6,365	121,262	−8.06° to 39.21°	−35.44° to −14.33°	0.164–11.9	16
9	Lajes–Thule	02/18/17 09:25	02/18/17 16:52	5,202	126,464	38.78° to 76.53°	−69.77° to −26.38°	0.173–9.60	14
10	Thule–Anchorage	02/19/17 16:25	02/20/17 00:02	4,654	131,118	61.17° to 80.52°	−157.44° to −68.78°	0.0571–10.7	12
11	Anchorage–Palmdale	02/21/17 18:01	02/21/17 23:48	4,629	135,747	34.63° to 61.17°	−150.09° to −117.75°	0.175–12.0	10
ATom-3									
1	Palmdale–equator–Palmdale	09/28/17 14:36	09/29/17 00:53	8,166	143,913	−0.39° to 34.71°	−121.64° to −117.73°	0.173–12.8	10
2	Palmdale–Anchorage	10/01/17 16:06	10/02/17 02:05	6,942	150,855	34.60° to 72.73°	−157.18° to −118.09°	0.0429–12.0	14
3	Anchorage–Kona	10/04/17 17:59	10/05/17 01:23	5,293	156,148	19.74° to 61.27°	−162.85° to −150.02°	0.0737–12.6	12
4	Kona–Nadi	10/06/17 18:56	10/07/17 03:51	6,683	162,831	−17.92° to 19.73°	−183.00° to −156.05°	0.171–12.6	16

Table ES2. Continued.

5	Nadi–Christchurch	10/08/17 20:01	10/09/17 5:13	6,529	169,360	−55.94° to −17.77°	−194.93° to −175.19°	0.154–12.2	18
6	Christchurch–Punta Arenas	10/11/17 17:57	10/12/17 03:50	7,862	177,222	−65.28° to −43.50°	−187.55° to −70.36°	0.168–11.7	16
7	Punta Arenas–Antarctica–Punta Arenas	10/14/17 11:35	10/14/17 22:15	7,771	184,993	−80.12° to −52.96°	−70.97° to −19.64°	0.165–12.0	16
8	Punta Arenas–Ascension Island	10/17/17 09:57	10/17/17 19:25	7,421	192,414	−53.00° to −7.75°	−70.94° to −14.38°	0.173–13.2	12
9	Ascension Island–Cabo Verde	10/19/17 08:36	10/19/17 13:10	3,146	195,560	−8.037° to 16.732°	−22.95° to −14.37°	0.171–12.9	8
10	Cabo Verde–Lajes	10/20/17 09:18	10/20/17 16:59	5,252	200,812	9.14° to 39.19°	−27.73° to −22.94°	0.165–12.4	12
11	Lajes–Bangor	10/23/17 09:33	10/23/17 18:59	6,729	207,541	38.57° to 67.01°	−68.96° to −26.82°	0.155–12.6	20
12	Bangor–Anchorage	10/25/17 14:02	10/25/17 23:36	7,011	214,552	44.67° to 79.99°	−151.02° to −67.74°	0.0687–12.3	16
13	Anchorage–Palmdale	10/27/17 18:24	10/28/17 00:53	4,356	218,908	34.58° to 61.18°	−150.13° to −118.09°	0.168–12.5	14
ATom-4									
1	Palmdale–equator–Palmdale	04/24/18 14:45	04/25/18 00:15	7,321	226,229	3.53° to 34.72°	−121.75° to −117.67°	0.166–12.4	10
2	Palmdale–Anchorage	04/27/18 16:03	04/28/18 02:23	7,254	233,483	34.61° to 72.64°	−157.36° to −117.94°	0.0444–11.4	14
3	Anchorage–Kona	04/29/18 17:55	04/30/18 02:02	5,417	238,900	19.53° to 61.17°	−162.87° to −150.00°	0.0707–11.8	12
4	Kona–Nadi	05/01/18 18:55	05/02/18 03:06	5,572	244,472	−17.95° to 19.73°	−182.79° to −156.05°	0.165–12.4	14
5	Nadi–Christchurch	05/03/18 20:58	05/04/18 04:51	5,035	249,507	−49.98° to −17.77°	−190.51° to −177.64°	0.163–12.0	16
6	Christchurch–Punta Arenas	05/06/18 20:21	05/07/18 06:29	7,816	257,323	−65.27° to −43.42°	−187.45° to −70.61°	0.171–11.9	16
7	Punta Arenas–Antarctica–Punta Arenas	05/09/18 11:53	05/09/18 22:37	7,947	265,270	−86.18° to −53.00°	−70.94° to −40.05°	0.172–11.6	13
8	Punta Arenas–Recife	05/12/18 11:28	05/12/18 21:26	7,237	272,507	−53.00° to −6.90°	−70.96° to −26.49°	0.160–12.2	16
9	Recife–Lajes	05/14/18 10:28	05/14/18 19:52	6,625	279,132	−8.20° to 38.96°	−34.92° to −23.16°	0.171–12.8	16
10	Lajes–Kangerlussuaq	05/17/18 09:28	05/17/18 19:09	7,323	286,455	38.77° to 75.94°	−66.94° to −14.43°	0.159–11.2	12
	Kangerlussuaq–Bangor *ferry flight*	05/18/18 12:21	05/18/18 15:32						
11	Bangor–Anchorage	5/19/18 14:02	5/20/18 00:39	7,441	293,896	44.77° to 82.94°	−150.23° to −68.53°	0.165–12.1	14
12	Anchorage–Palmdale	05/21/18 16:47	05/21/18 23:37	7,209	301,105	34.63° to 61.26°	−150.31° to −117.95°	0.176–12.3	12

Table ES3. Total flight time of the individual research flights and the percentage of each flight spent within the four altitude layers noted in Fig. ES4: marine boundary layer (MBL), MBL to 500-mb pressure altitude, 500 mb to the tropopause, and stratosphere.

Flight No.	Location	Flight time (min)	Time MBL (%)	Time MBL–500 mb (%)	Time 500 mb–tropopause (%)	Time stratosphere (%)
ATom-1						
1	Palmdale–equator–Palmdale	563	9.4	29.5	61.1	0.0
2	Palmdale–Anchorage	618	4.7	17.6	67.5	10.4
3	Anchorage–Kona	441	6.1	31.5	59.9	2.5
4	Kona–American Samoa	526	15.4	32.7	51.9	0.0
5	American Samoa–Christchurch	402	10.7	33.8	37.3	18.2
6	Christchurch–Punta Arenas	651	9.5	24.1	48.8	17.5
7	Punta Arenas–Ascension Island	570	14.4	23.5	53.2	8.9
8	Ascension Island–Lajes	520	11.9	32.7	55.4	0.0
9	Lajes–Kangerlussuaq	596	4.7	28.2	51.3	15.8
10	Kangerlussuaq–Minneapolis	361	10.5	34.6	42.7	12.2
11	Minneapolis–Palmdale	298	8.4	31.5	60.1	0.0
ATom-2						
1	Palmdale–equator–Palmdale	631	8.2	16.5	69.3	4.4
2	Palmdale–Anchorage	594	5.1	28.8	36.4	27.8
3	Anchorage–Kona	498	14.1	35.3	50.6	0.0
4	Kona–Fiji	574	11.0	23.3	65.7	0.0
5	Fiji–Christchurch	520	10.6	24.0	52.7	12.7
6	Christchurch–Punta Arenas	600	7.3	18.8	37.8	36.0
7	Punta Arenas–Ascension Island	555	9.7	14.6	75.7	0.0
8	Ascension Island–Lajes	533	13.5	27.0	59.5	0.0
9	Lajes–Thule	459	2.2	33.3	51.0	10.9
10	Thule–Anchorage	473	4.2	42.9	15.4	37.4
11	Anchorage–Palmdale	368	15.5	25.5	26.9	32.1
ATom-3						
1	Palmdale–equator–Palmdale	626	6.2	16.9	76.8	0.0
2	Palmdale–Anchorage	615	7.2	28.5	57.1	7.3
3	Anchorage–Kona	450	14.0	26.7	59.3	0.0
4	Kona–Fiji	541	12.9	27.4	59.7	0.0
5	Fiji–Christchurch	557	10.4	28.0	51.3	10.2
6	Christchurch–Punta Arenas	600	8.8	24.2	32.5	34.5
7	Punta Arenas–Antarctica–Punta Arenas	649	7.7	19.9	66.9	5.5
8	Punta Arenas–Ascension Island	576	8.7	20.0	71.0	0.3
9	Ascension Island–Cabo Verde	282	14.5	30.9	54.6	0.0
10	Cabo Verde–Lajes	469	19.4	24.7	55.9	0.0
11	Lajes–Bangor	573	13.1	34.9	52.0	0.0
12	Bangor–Anchorage	585	5.1	35.0	35.2	24.6
13	Anchorage–Palmdale	396	11.6	35.4	53.0	0.0
ATom-4						
1	Palmdale–equator–Palmdale	570	6.1	18.6	75.3	0.0
2	Palmdale–Anchorage	620	6.9	31.9	34.8	26.3
3	Anchorage–Kona	487	10.5	34.5	55.0	0.0
4	Kona–Fiji	491	14.5	30.8	54.8	0.0
5	Fiji–Christchurch	473	12.3	35.7	45.0	7.0
6	Christchurch–Punta Arenas	608	6.3	27.5	33.7	32.6
7	Punta Arenas–Antarctica–Punta Arenas	644	3.7	26.1	22.8	48.3
8	Punta Arenas–Recife	598	10.9	28.3	54.8	6.0
9	Recife–Lajes	564	9.0	30.	57.6	2.5
10	Lajes–Kangerlussuaq	581	4.8	25.6	41.7	27.9
11	Bangor–Anchorage	637	7.7	25.4	39.1	27.8
12	Anchorage–Palmdale	410	9.	38.5	38.5	13.4

Table ES4. List of published articles to date using data collected from the ATom mission.

Publications to date using ATom data
Anderson, D., et al. (2021), Spatial and temporal variability in the hydroxy (OH) radical: understanding the role of large-scale climate features and their influence on OH through its dynamical and photochemical drivers, *Atmos. Chem. Phys.*, 21, 6481–6508, doi:10.5194/acp-21-6481-2021.
Asher, E., et al. (2019), Novel approaches to improve estimates of short-lived halocarbon emissions during summer from the Southern Ocean using airborne observations, *Atmos. Chem. Phys.*, *19*, 14071–14090, doi:10.5194/acp-19-14071-2019.
Bates, K. H., et al. (2021), The Global Budget of Atmospheric Methanol: New Constraints on Secondary, Oceanic, and Terrestrial Sources, *J. Geophys. Res.*, *126*, doi:10.1029/2020JD033439.
Bian, H., et al. (2019), Observationally constrained analysis of sea salt aerosol in the marine atmosphere, *Atmos. Chem. Phys., 19*, 10773–10785, doi:10.5194/acp-2019-18.
Birner, B., et al. (2020), Gravitational separation of Ar/N2 and age of air in the lowermost stratosphere in airborne observations and a chemical transport model, *Atmos. Chem. Phys.*, doi:10.5194/acp-2020-95.
Bourgeois, I., et al. (2020), Global-scale distribution of ozone in the remote troposphere from ATom and HIPPO airborne field missions., *Atmos. Chem. Phys.*, doi:10.5194/acp-2020-315.
Brewer, J., et al. (2020), Evidence for an Oceanic Source of Methyl Ethyl Ketone to the Atmosphere, *J. Geophys. Res.*, 60273, Article, doi:10.1029/2019GL086045.
Brock, C., et al. (2019), Aerosol size distributions during the Atmospheric Tomography Mission (ATom): methods, uncertainties, and data products, *Atmos. Meas. Tech.*, 12, 3081–3099, doi:10.5194/amt-12-3081-2019.
Brock, C., et al. (2021), Ambient aerosol properties in the remote atmosphere from global scale in situ measurements, *Atmos. Chem. Phys.*, doi:10.5194/acp-2021-173.
Brune, W. H., et al. (2020), Exploring Oxidation in the Remote Free Troposphere: Insights From Atmospheric Tomography (ATom), *J. Geophys. Res.*, 125, doi:10.1029/2019JD031685.
Chen, X., et al. (2019), On the sources and sinks of atmospheric VOCs: an integrated analysis of recent aircraft campaigns over North America, *Atmos. Chem. Phys.*, 19, 9097–9123, doi:10.5194/acp-19-9097-2019.
Chen, X., et al. (2021), HCOOH in the remote atmosphere: Constraints from Atmospheric Tomography (ATom) 1 airborne observations, *ACS Earth and Space Chem.*, doi:10.1021/acsearthspacechem.1c00049.
Chen, Z., et al. (2021), Five years of variability in the global carbon cycle: comparing an estimate from the Orbiting Carbon Observatory-2 and process-based models, *Environ. Res. Lett.*, 16, doi:10.1088/1748-9326/abfac1.
Chen, Z., et al. (2021), Linking global terrestrial CO2 fluxes and environmental drivers: inferences from the Orbiting Carbon Observatory-2 satellite and terrestrial biospheric models, *Atmos. Chem. Phys.*, 21, 6663–6680, doi:10.5194/acp-21-6663-2021.
Chevallier, F., et al. (2019), Objective evaluation of surface- and satellite-driven carbon dioxide atmospheric inversions, *Atmos. Chem. Phys.*, 19, 14233–14251, doi:10.5194/acp-19-14233-2019.
Crowell, S., et al. (2019), The 2015–2016 carbon cycle as seen from OCO-2 and the global in situ network, *Atmos. Chem. Phys.*, 19, 9797–9831, doi:10.5194/acp-19-9797-2019.
Deeter, M., et al. (2019), Radiance-based retrieval bias mitigation for the MOPITT instrument: the version 8 product, *Atmos. Meas. Tech.*, 12, 4561–4580, doi:10.5194/amt-12-4561-2019.
DeMott, P. J., et al. (2021), Machine learning uncovers aerosol size information from chemistry and meteorology to quantify potential cloud-forming particles.
Ditas, J., et al. (2018), Strong impact of wildfires on the abundance and aging of black carbon in the lowermost stratosphere, *Proc. Natl. Acad. Sci.*, 811595–11603, doi:10.1073/pnas.1806868115.
Fisher, J. A., et al. (2018), Methyl, Ethyl, and Propyl Nitrates: Global Distribution and Impacts on Reactive Nitrogen in Remote Marine Environments, *J. Geophys. Res.*, 123, 12,429–12,451, doi:10.1029/2018JD029046.
Froyd, K., et al. (2019), A new method to quantify mineral dust and other aerosol species from aircraft platforms using single-particle mass spectrometry, *Atmos. Meas. Tech.*, 12, 6209–6239, doi:10.5194/amt-12-6209-2019.
Froyd, K, et al. (2021), Global-scale measurements reveal cirrus clouds are seeded by mineral dust aerosol, (in review).
Gonzalez, Y., et al. (2021), Impact of stratospheric air and surface emissions on tropospheric nitrous oxide during ATom, *Atmos. Chem. Phys.*, doi:10.5194/acp-2021-167.
Guo, H., et al. (2021), The Importance of Size Ranges in Aerosol Instrument Intercomparisons: A Case Study for the ATom Mission, *Atmos. Meas. Tech.*, doi:10.5194/amt-2020-224.
Hall, S. R., et al. (2018), Cloud impacts on photochemistry: building a climatology of photolysis rates from the Atmospheric Tomography mission, *Atmos. Chem. Phys.*, 18, 16809–16828, doi:10.5194/acp-18-16809-2018.
Hintsa, E. J., et al. (2021), UAS Chromatograph for Atmospheric Trace Species (UCATS) – a versatile instrument for trace gas measurements on airborne platforms, *Atmos. Meas. Tech.*, doi:10.5194/amt-2020-496.

Table ES4. Continued.

Hodshire, A., et al. (2019), The potential role of methanesulfonic acid (MSA) in aerosol formation and growth and the associated radiative forcings, *Atmos. Chem. Phys.*, 19, 3137–3160, doi:10.5194/acp-19-3137-2019.
Hodzic, A., et al. (2016), Rethinking the global secondary organic aerosol (SOA) budget: stronger production, faster removal, shorter lifetime, *Atmos. Chem. Phys.*, 16, 7917–7941, doi:10.5194/acp-16-7917-2016.
Hodzic, A., et al. (2020), Characterization of organic aerosol across the global remote troposphere: a comparison of ATom measurements and global chemistry models, *Atmos. Chem. Phys.*, 20, 4607–4635, doi:10.5194/acp-20-4607-2020.
Jin, Y., et al. (2021), A mass-weighted isentropic coordinate for mapping chemical tracers and computing atmospheric inventories, *Atmos. Chem. Phys.*, 21, 217–238, doi:10.5194/acp-21-217-2021.
Katich, J., et al. (2018), Strong Contrast in Remote Black Carbon Aerosol Loadings Between the Atlantic and Pacific Basins, *J. Geophys. Res.*, 123, 13,386–13,395, doi:10.1029/2018JD029206.
Koenig, T., et al. (2020), Quantitative detection of iodine in the stratosphere, *Proc. Natl. Acad. Sci.*, 117, doi:10.1073/pnas.1916828117.
Kulawik, S., et al. (2021), Evaluation of single-footprint AIRS CH4 profile retrieval uncertainties using aircraft profile measurements, *Atmos. Meas. Tech.*, 14, 335–354, doi:10.5194/amt-14-335-2021.
Kupc, A., et al. (2018), Modification, calibration, and performance of the Ultra-High Sensitivity Aerosol Spectrometer for particle size distribution and volatility measurements during the Atmospheric Tomography Mission (ATom) airborne campaign, *Atmos. Meas. Tech.*, 11, 369–383, doi:10.5194/amt-11-369-2018.
Kupc, A., et al. (2020), The potential role of organics in new particle formation and initial growth in the remote tropical upper troposphere, *Atmos. Chem. Phys.*, 20, 15037–15060, doi:10.5194/acp-20-15037-2020.
Lamb, K., et al. (2021), Global-scale constraints on light-absorbing anthropogenic iron oxide aerosols, *Nature*, doi:10.1038/s41612-021-00171-0.
Liu, J., et al. (2021), Carbon Monitoring System Flux Net Biosphere Exchange 2020 (CMS-Flux NBE 2020), *Earth Syst. Sci. Data*, 13, 299–330, doi:10.5194/essd-13-299-2021.
Liu, S., et al. (2021), Sea spray aerosol concentration modulated by sea surface temperature, *Proc. Natl. Acad. Sci.*, doi:10.1073/pnas.2020583118.
Lou, S., et al. (2020), New SOA Treatments Within the Energy Exascale Earth System Model (E3SM): Strong Production and Sinks Govern Atmospheric SOA Distributions and Radiative Forcing, *J. Adv. Modeling Earth Syst.*, 12, e2020MS002266, doi:10.1029/2020MS002266.
Lu, X., et al. (2021), Global methane budget and trend, 2010–2017: complementarity of inverse analyses using in situ (GLOBALVIEWplus CH4 ObsPack) and satellite (GOSAT) observations, *Atmos. Chem. Phys.*, 21, 4637–4657.
Lund, M. T., et al. (2019), Short Black Carbon lifetime inferred from a global set of aircraft observations, *Nature Clim. Atmos. Sci.*, doi:10.1038/s41612-018-0040-x.
Luo, G., F. Yu, and J. M. Moch (2020), Further improvement of wet process treatments in GEOS-Chem v12.6.0: impact on global distributions of aerosols and aerosol precursors, *Geosci. Model. Dev.*, 13, 2879–2903, doi:10.5194/gmd-13-2879-2020.
Martínez-Alonso, S., et al. (2020), 1.5 years of TROPOMI CO measurements: comparisons to MOPITT and ATom, *Atmos. Meas. Tech.*, 13, 4841–4864, doi:10.5194/amt-13-4841-2020.
Murphy, D., et al. (2018), An aerosol particle containing enriched uranium encountered in the remote T upper troposphere, *Journal of Environmental Radioactivity*, 184–185, 95–100, doi:10.1016/j.jenvrad.2018.01.006.
Murphy, D., et al. (2019), The distribution of sea-salt aerosol in the global troposphere, *Atmos. Chem. Phys.*, 19, 4093–4104, doi:10.5194/acp-19-4093-2019.
Murphy, D., et al. (2021), Radiative and chemical implications of the size and composition of aerosol particles in the existing or modified global stratosphere, *Atmos. Chem. Phys.*, doi:10.5194/acp-2020-909.
Nair, A. et al. (2021), Machine learning uncovers aerosol size information from chemistry and meteorology to quantify potential cloud-forming particles. *Geophys. Res. Lett.*, **48**, e2021GL094133, doi:10.1029/2021GL094133.
Nalli, N., et al. (2020), Validation of Carbon Trace Gas Profile Retrievals from the NOAA-Unique Combined Atmospheric Processing System for the Cross-Track Infrared Sounder, *Remote Sens.*, 12, doi:10.3390/rs12193245.
Nault, B., et al. (2020), Interferences with aerosol acidity quantification due to gas-phase ammonia uptake onto acidic sulfate filter samples, *Atmos. Meas. Tech.*, 13, 6193–6213, doi:10.5194/amt-13-6193-2020.
Nault, B., et al. (2021), Chemical transport models often underestimate inorganic aerosol acidity in remote regions of the atmosphere, *Commun. Earth Environ.*, 2, doi:10.1038/s43247-021-00164-0.
Naus, S., et al. (2021), A 3D-model inversion of methyl chloroform to constrain the atmospheric oxidative capacity, *Atmos. Chem. Phys.*, doi:10.5194/acp-2020-624.
Pai, S. J., et al. (2020), An evaluation of global organic aerosol schemes using airborne observations, *Atmos. Chem. Phys.*, 20, 2637–2665, doi:10.5194/acp-2019-331.

Table ES4. Continued.

Pieber, S. M., et al. (2016), Inorganic Salt Interference on CO2 + in Aerodyne AMS and ACSM Organic Aerosol Composition Studies, *Environ. Sci. Technol.*, 50, 10494–10503, doi:10.1021/acs.est.6b01035.
Prather, M., et al. (2017), Global atmospheric chemistry – which air matters, *Atmos. Chem. Phys.*, 17, 9081–9102, doi:10.5194/acp-17-9081-2017.
Prather, M., et al. (2018), How well can global chemistry models calculate the reactivity of short-lived greenhouse gases in the remote troposphere, knowing the chemical composition, *Atmos. Meas. Tech.*, 11, 2653–2668, doi:10.5194/amt-11-2653-2018.
Ranjthkumar, A., et al. (2021), Constraints on global aerosol number, SO2, and condensation sink in UKESM1 using ATom measurements, *Atmos. Chem. Phys.*, 21, 4979–5014, doi:10.5194/acp-21-4979-2021.
Rickly, P., et al. (2021), Improvements to a laser-induced fluorescence instrument for measuring SO2 – impact on accuracy and precision, *Atmos. Meas. Tech.*, 14, 2429–2439, doi:10.5194/amt-14-2429-2021.
Schill, G., et al. (2020), Widespread biomass burning smoke throughout the remote troposphere, *Nature Geoscience*, doi:10.1038/s41561-020-0586-1.
Schueneman, M., et al. (2021), Aerosol pH Indicator and Organosulfate Detectability from Aerosol Mass Spectrometry Measurements, *Atmos. Meas. Tech.*, doi:10.5194/amt-2020-339.
Spanu, A., et al. (2019), Flow-induced errors in airborne in situ measurements of aerosols and clouds, *Atmos. Meas. Tech.*, 2019, doi:10.5194/amt-2019-27.
St. Clair, J. M., et al. (2019), CAFE: a new, improved nonresonant laser-induced fluorescence instrument for airborne in situ measurement of formaldehyde, *Atmos. Meas. Tech.*, 12, 4581–4590, doi:10.5194/amt-12-4581-2019.
Stephens, B., et al. (2020), Airborne measurements of oxygen concentration from the surface to the lower stratosphere and pole to pole, *Atmos. Meas. Tech.*, doi:10.5194/amt-2020-294.
Strode, S., et al. (2018), Forecasting carbon monoxide on a global scale for the ATom-1 aircraft mission: insights from airborne and satellite observations and modeling, *Atmos. Chem. Phys.*, 18, 10955–10971, doi:10.5194/acp-18-10955-2018.
Thames, A., et al. (2020), Missing OH reactivity in the global marine boundary layer, *Atmos. Chem. Phys.*, 20, 4013–4029, doi:10.5194/acp-20-4013-2020.
Tilmes, S., et al. (2019), Climate Forcing and Trends of Organic Aerosols in the Community Earth System Model (CESM2), *J. Adv. Modeling Earth Syst.*, 11, 4323–4351, doi:10.1029/2019MS001827.
Travis, K., et al. (2020), Constraining remote oxidation capacity with ATom observations, *Atmos. Chem. Phys.*, 20, 7753–7781, doi:10.5194/acp-20-7753-2020.
Veres, P., et al. (2020), Global airborne sampling reveals a previously unobserved dimethyl sulfide oxidation mechanism in the marine atmosphere, *Proc. Natl. Acad. Sci.*, 117, doi:10.1073/pnas.1919344117.
Wang, S., et al. (2019), Ocean Biogeochemistry Control on the Marine Emissions of Brominated Very Short-Lived Ozone-Depleting Substances: A Machine-Learning Approach, *J. Geophys. Res.*, 124, doi:10.1029/2019JD031288.
Wang, S., et al. (2019), Atmospheric Acetaldehyde: Importance of Air-Sea Exchange and a Missing Source in the Remote Troposphere, *Geophys. Res. Lett.*, 46, doi:10.1029/2019GL082034.
Wang, S., et al. (2020), Global Atmospheric Budget of Acetone: Air-Sea Exchange and the Contribution to Hydroxyl Radicals, *J. Geophys. Res.*, 125, e2020JD032553, doi:10.1029/2020JD032553.
Williamson, C., et al. (2018), Fast time response measurements of particle size distributions in the 3–60 nm size range with the nucleation mode aerosol size spectrometer, *Atmos. Meas. Tech.*, 11, 3491–3509, doi:10.5194/amt-11-3491-2018.
Williamson, C., et al. (2019), A large source of cloud condensation nuclei from new particle formation in the tropics, *Nature*, 574, 399–403, doi:10.1038/s41586-019-1638-9.
Williamson, C., et al. (2021), Large hemispheric difference in nucleation mode aerosol concentrations in the lowermost stratosphere at mid and high latitudes, *Atmos. Chem. Phys.*, doi:10.5194/acp-2021-22.
Wolfe, G. M., et al. (2019), Mapping hydroxyl variability throughout the global remote troposphere via synthesis of airborne and satellite formaldehyde observations, *Proc. Natl. Acad. Sci.*, doi:10.1073/pnas.1821661116.
Yu, P., et al. (2019), Efficient In-Cloud Removal of Aerosols by Deep Convection, *Geophys. Res. Lett.*, 46, 1061–1069, doi:10.1029/2018GL080544.
Yu, X., et al. (2021), Aircraft-based inversions quantify the importance of wetlands and livestock for Upper Midwest methane emissions, *Atmos. Chem. Phys.*, 21, 951–971, doi:10.5194/acp-21-951-2021.
Zeng, L., et al. (2020), Global Measurements of Brown Carbon and Estimated Direct Radiative Effects, *Geophys. Res. Lett.*, 47, doi:10.1029/2020GL088747.
Zhu, L., et al. (2019), Effect of sea salt aerosol on tropospheric bromine chemistry, *Atmos. Chem. Phys.*, 19, 6497–6507, doi:10.5194/acp-19-6497-2019.
Zhu, L., et al. (2020), Validation of satellite formaldehyde (HCHO) retrievals using observations from 12 aircraft campaigns, *Atmos. Chem. Phys.*, 20, 12329–12345, doi:10.5194/acp-20-12329-2020.

Table ES5. Project management and science team members involved in the ATom mission.

Team	Team members
Project leadership	
Principal investigator	Steven C. Wofsy
Deputy principal investigator	Michael J. Prather
Mission science	Thomas B. Ryerson, Paul A. Newman, Thomas F. Hanisco, David W. Fahey, Paul O. Wennberg
Project management	
Project manager	Dave Jordan
Deputy project manager	Erin P. Czech
Project coordinator	Liz Juvera
Data manager	Katja Drdla
Site managers	Quincy Allison, Dan Chirica, Bernie Luna, Vidal Salazar, Marilyn Vasques, Jhony Zavaleta
Site support	Susan McFadden, Sommer Nicholas, Brent Allan Williams
Logistics	Quincy Allison, Drew Thompson
Instrument teams	
AMP	Charles A. Brock, Agnieszka Kupc, Christina J. Williamson, Frank Erdesz
AO2/Medusa	Britton B. Stephens, Eric J. Morgan, Ralph F. Keeling, Andrew S. Watt, Jonathan D. Bent, William Paplawsky, Sara Afshar
ATHOS	William H. Brune, David O. Miller, Alexander B. Thames
CAFS	Samuel R. Hall, Kirk Ullmann
CAPS	Bernadett Weinzierl, Maximilian Dollner, Harald Schuh, Nikolaus Foelker
CIT-CIMS	Michelle J. Kim, Hannah M. Allen, John D. Crounse, Paul O. Wennberg, Alexander P. Tang, Lu Xu
DLH	Glenn S. Diskin, Joshua DiGangi
GT-CIMS	L. Gregory Huey, David Tanner
CU HR-AMS	Jose L. Jimenez, Pedro Campuzano-Jost, Benjamin A. Nault, Alma Hodzic, Douglas A. Day, Jason C. Schroder, Derek J. Price, Donna Sueper, David S. Thompson, Hongyu Guo, Melinda K. Schueneman
ISAF/CANOE	Thomas F. Hanisco, Glenn M. Wolfe, Jason M. St. Clair, Julie M. Nicely, Reem A. Hannun, Andrew K. Swanson, Jin Liao
MMS	T. Paul Bui, Cecilia Chang
NOAA Picarro	Kathryn McKain, Colm Sweeney, Tim Newberger, Sonja Wolter
NOAA ToF-CIMS	Patrick R. Veres, Jonathan A. Neuman
NOyO3	Thomas B. Ryerson, Chelsea R. Thompson, Jeff Peischl, Ilann Bourgeois, Ken Aikin, Rich McLaughlin
PALMS	Karl Froyd, Daniel M. Murphy, Gregory Schill
PANTHER/UCATS	James Elkins, Eric Hintsa, Fred Moore, Geoff Dutton, Brad Hall
PFP	Stephen Montzka, Ben Miller
QCLS	Steven C. Wofsy, Róisín Commane, Bruce Daube, John Budney, Maryann Sargent, Yenny Gonzalez Ramos, Eric Kort
SAGA	Jack Dibb, Rodney Weber, Linghan Zeng, Eric Scheuer
SO2 LIF	Andrew Rollins
SOAP	Nicholas Wagner
SP2	Joshua P. Schwarz, Joseph M. Katich, Kara Lamb
TOGA	Eric Apel, Rebecca Hornbrook, Siyuan Wang, Alan Hills, Elizabeth Asher
WAS	Donald Blake, Simone Meinardi, Nicola Blake, Barbara Barletta
Forecasting and modeling teams	
Mission meteorology	Karen Rosenlof, Amy Butler, Eric Ray, Leslie Lait, Xiaohua Pan, Mian Chin
NASA Goddard Space Flight Center modelers	Sarah A. Strode, Stephen D. Steenrod, Junhua Liu, Huisheng Bian, Susan Strahan, Megan Damon
University of California, Irvine, modelers	Michael J. Prather, Hao Guo, Clare M. Flynn
NCAR modelers	Jean-Francois Lamarque, Forrest Lacey, Louisa Emmons
Lamont-Doherty Earth Observatory modelers	Arlene M. Fiore, Gus Correa
University of Rochester modelers	Lee T. Murray